Performance Comparison of FIR Low-Pass Digital Differentiators for Measurement Applications

David Macii, Dario Petri
University of Trento - Dep. of Industrial Engineering
Trento, Italy
Email: david.macii@unitn.it

***Abstract*—Low-pass Digital Differentiators (LPDs) are adopted in a variety of measurement and testing applications. However, a clear performance analysis of different solutions is seldom reported in the scientific literature. Maybe this is due to the lack of criteria to analyze their behavior on a common basis. In this paper, the passband and stopband features of two families of Finite Impulse Response (FIR) LPDs (namely those resulting from the classic windowing design method and the so-called maximally-flat differentiators) are purposely analyzed under comparable conditions. In particular, starting from a revised definition of Equivalent Noise Bandwidth (ENBW) adapted to the LPD case, a criterion to compare both types of digital differentiators is proposed for common settings of ENBW and impulse response length. The reported analysis shows that, even if the maximally-flat LPDs exhibit a smoother frequency response within the passband, a negligible magnitude error around DC and the possibility to compute the coefficients using recursive analytical expressions, they are less selective than the corresponding windowing-based differentiators. Moreover, while the stopband attenuation of maximally-flat LPDs is higher, their Root Mean Square (RMS) magnitude response errors within the passband are significantly higher. Last but not least, the maximally-flat LPDs suffer from two crucial problems, i.e. finite (and potentially coarse) bandwidth resolution and poor numerical stability, as the filter order grows.**

Keywords*—*Digital differentiators, Finite Impulse Response (FIR) filters, digital filter design, performance evaluation, power systems frequency estimation

I. Introduction

Integer and fractional-order digital differentiators are used in a variety of applications, such as robot control [1], biomedical (e.g., electrocardiogram) signal preprocessing [2], seismic signal analysis [3], and dynamic synchrophasor or frequency estimation in power systems [4]–[6]. For this reason, the design of digital differentiators has been an active topic of research for many years [7], [8]. Various kinds of Infinite Impulse Response (IIR) or Finite Impulse Response (FIR) filters have been proposed to differentiate discrete-time signals while drastically reducing noise and disturbances. In general, a maximally-flat frequency response is highly desirable if the spectral content of the signal to be differentiated is concentrated around DC [7]. However, ensuring a maximally-flat frequency response with low-pass selectivity through a single filter (i.e. not resulting from the cascade of a standard differentiator and a classic low-pass filter) requires a careful design. In [9] a regression analysis based on orthogonal polynomials in the time domain is used to derive closed-form expressions for maximally-flat IIR smoothers or differentiators with tunable features. Even though it is shown in [10] that low-order IIR Low-Pass Digital Differentiators (LPDs) with an almost linear phase response can be designed, the FIR solutions are preferable to the IIR ones since they exhibit a perfectly linear phase response over the whole passband. An effective approach to design computationally-efficient fractional-order digital FIR differentiators able to mitigate the detrimental effect of wide-band noise is described in [11]. In [12] a weighted least squares estimator applied to a signal model approximated by its Taylor's series leads to the identification of a bank of FIR differentiators with a maximally-flat frequency response within the passband. However, these differentiators are not conceived to filter the noise outside a given bandwidth. A recursive expression enabling the computation of the impulse response coefficients of maximally-flat FIR LPDs is instead reported in [13]. The possibility to compute the filter coefficients with closed-form expressions as well as the very small magnitude error around DC are indeed the main advantages of this kind of LPDs. However, to the best of Authors' knowledge, the actual frequency selectivity of this kind of filters as well as their advantages with respect to other more standard solutions is not clearly reported in the scientific literature. The purpose of this paper is to partly fill this gap by analyzing if, and to what extent, the FIR maximally-flat LPDs are preferable to those obtained by using the classic windowing design method.

The rest of this paper is structured as follows. First, in Section II the main steps needed to design either an LPD based on the windowing method or a maximally-flat FIR LPD are briefly recalled. Also, the definition of filter Equivalent Noise Bandwidth (ENBW) is revised and adapted to the LPD case. In Section III the passband and stopband features of the two families of LPD filters mentioned above are compared for common values of ENBW and impulse response length. Section IV reports a performance comparison between the two kinds of filters in a practical application, i.e. for voltage frequency estimation in power systems [6], [14], [15]. Finally, Section V concludes the paper.

II. Theoretical Background

A digital LPD is a discrete-time filter, whose ideal frequency response in the domain of normalized frequency $\omega \in [-\pi, \pi]$ is

$$H_{id}(e^{j\omega}) = \begin{cases} j\omega & |\omega| \leq \omega_c \\ 0 & \omega_c < |\omega| \leq \pi \end{cases} \quad (1)$$

where ω_c is the cut-off frequency of the filter (expressed in radians) and $\omega = \pi$ corresponds to the Nyquist frequency. Of course, an LPD based on (1) is neither causal, nor physically realizable, as its impulse response spans from $-\infty$ to $+\infty$. Thus, (1) has to be properly approximated to implement a feasible LPD. As briefly explained in the Introduction, two different solutions for FIR LPD design are considered and compared in this paper. The former one is based on the classic windowing method, whereas the latter ensures a maximally-flat behavior around DC. This means that the first derivative of the magnitude response at $\omega = 0$ is 1, while both the frequency response itself and its higher derivatives from 2 till a given finite order are null at $\omega = 0$. For the sake of simplicity and without loss of generality, the case of FIR LPDs with a perfectly antisymmetric impulse response with respect to time $n = 0$ (namely with a constant phase response equal to $\pi/2$ for $\omega > 0$ and $-\pi/2$ for $\omega < 0$) will be considered in the following. However, the results of the proposed analysis hold also in the case of causal, linear-phase LPDs.

A. FIR LPD design based on the windowing method

The windowing method is a classic FIR design technique, which simply relies on the truncation to N coefficients of the impulse response of the corresponding ideal filter. Thus, N must be chosen in such a way as to preserve most of the impulse response energy. Unfortunately, due to the so-called Gibbs phenomenon, the magnitude of the frequency response ripples located around the cut-off frequency of the ideal filter do not decrease as N grows. However, their magnitude can be reduced by weighing the truncated impulse response with the coefficients of a suitable window function, most notably a cosine-class window or the so-called Kaiser window.

In the case at hand, by computing the Inverse Discrete-Time Fourier Transform (IDTFT) of (1), the impulse response of an FIR LPD of order N (assuming, without loss of generality, that N is odd) is given by:

$$h(n) = \left[\frac{\omega_c}{\pi n}\cos\omega_c n - \frac{1}{\pi n^2}\sin\omega_c n\right] w(n) \qquad (2)$$

where $n = -\frac{N-1}{2}, \ldots, \frac{N-1}{2}$ and $w(n)$ is the chosen window function.

B. Maximally-flat FIR LPD design

The design procedure of a maximally-flat FIR LPD relies on the power series expansion of its transfer function within the Nyquist frequency [16]. In particular, considering that an FIR LPD must be either a Type III or Type IV system, its transfer function must include at least one zero at DC (i.e. for $z = 1$) and a variable number of zeros at frequency $\omega = \pi$ (i.e. for $z = -1$). Therefore, after several algebraic steps, it can be shown that the transfer function of maximally-flat FIR LPDs is [13]

$$H(z) = \left(\frac{1-z^{-1}}{2}\right)\left(\frac{1+z^{-1}}{2}\right)^K z^{-L}\sum_{n=0}^{L} c(n)\left(\frac{-z+2-z^{-1}}{4}\right)^n \qquad (3)$$

where, for a given filter order N, $K \leq N-2$ denotes the number of zeros of the transfer function at $z = -1$, $L = \frac{(N-K)}{2} - 1$ must be integer and determines the maximum order of the derivatives of the magnitude response that are null at DC, and finally coefficients $c(\cdot)$ are computed through the following recursive expression [13], i.e.

$$c(n) = \frac{(8n^2+4Kn-10n-K+3)c(n-1)-(2n+K-3)^2 c(n-2)}{2n(2n+1)} \qquad (4)$$

where $c(0) = 2$ and $c(1) = K + 1/3$. Of course, for given values of N and K, the impulse response $h(n)$ of the maximally-flat FIR LPD results simply from the inverse $Z-$transform of (3). It is worth noticing that the bandwidth of these LPDs depends on the values of L (or K) and N, as it will be clearly shown in Section II-C. For $K = 0$, a full-band differentiator is obtained. On the contrary, as K increases (namely if L tends to 0), the LPD bandwidth decreases, thus reaching its minimum for $K = N - 2$. Moreover, given that both K and N must be integer numbers, the possible bandwidth values are discretized with a resolution that improves with N.

C. ENBW definition in the LPD case

From expressions (2) and (3)-(4) it is quite evident that the the features of windowing-based and maximally-flat FIR LPDs depend on two different pairs of parameters, i.e. (N, ω_c) and (N, L) [or (N, K)], respectively. Therefore, besides the filter order N, an additional condition must be set to enable a fair comparison between these two kinds of LPDs. Unfortunately, no analytical expressions exist to relate ω_c with L (or K). Moreover, ω_c delimits just the theoretical passband of an ideal LPD, which is inherently different from the bandwidth of the real filter. To overcome this conceptual problem, in the following, the windowing-based and the maximally-flat LPDs of the same order are compared assuming that they have the same ENBW value. In Authors' opinion, this choice is absolutely reasonable, since the role common to all LPDs is to compute the derivative of an input signal that is usually corrupted by wideband noise. In general, the ENBW of a filter is defined as the one-sided or two-sided bandwidth of the ideal filter that returns the same output power as the filter considered, when both filters are stimulated by the same white noise. Even though this definition was originally conceived for classic low-pass or band-pass filters, it can be extended and adapted to the LPD case. In particular, by applying the definition above to the frequency response of an ideal LPD and recalling the Parseval's theorem, it follows that

$$\frac{1}{\pi}\int_0^{ENBW} \omega^2 d\omega = \frac{1}{\pi}\int_0^{\pi} |H(e^{j\omega})|^2 d\omega = \sum_{n=-\frac{N-1}{2}}^{\frac{N-1}{2}} h^2(n), \qquad (5)$$

where $|H(e^{j\omega})|$ and $h(n)$ denote the magnitude response and the impulse response, respectively, of the real LPD considered. Hence, by solving the leftmost integral in (5), the LPD one-sided ENBW is given by

$$ENBW = \sqrt[3]{3\pi \sum_{k=-\frac{N-1}{2}}^{\frac{N-1}{2}} h^2(k)}. \qquad (6)$$

Although the values returned by (6) are in radians and lie within the interval $[0, \pi]$, for the sake of clarity the ENBW values normalized by π will be shown in the rest of this paper.

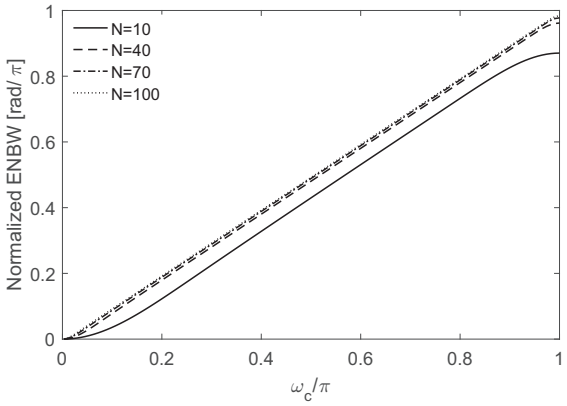

(a)

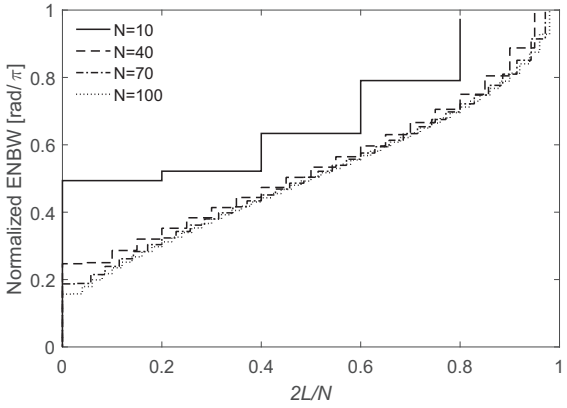

(b)

Fig. 1. Normalized ENBW of the windowing-based FIR LPDs (using the Hann window) (a) and the maximally-flat ones (b), for the same impulse response length (i.e., $N = 10, 40, 70, 100$), while varying the respective design parameters (i.e., ω_c/π in (a) and $2L/N$ in (b)).

Fig. 1(a)-(b) shows the normalized ENBW values for LPDs of the same order obtained with the windowing method (using the Hann window) and the maximally-flat design approach, respectively. Different line styles refers to distinct N values (i.e., $N = 10, 40, 70, 100$). The normalized ENBW values are plotted as a function of the respective design parameters over the same normalized scale, i.e. ω_c/π in Fig. 1(a) and $2L/N$ in Fig. 1(b). The ENBW of the windowing-based LPDs almost coincides with the ideal LPD bandwidth when $N \geq 40$ (as expected) and it can be finely set by tuning ω_c, unless the wanted bandwidth is very narrow (< 0.1 rad/π) or very broad (> 0.9 rad/π). The results obtained with higher-order Maximum-Sidelobe Decay (MSD) windows are very similar to those shown in Fig. 1(a) and are not plotted for the sake of brevity.

The normalized ENBW of maximally-flat LPDs depends on both N and L. From a design perspective, we found through numerical interpolation that, for a given value of $N \geq 40$, the integer value of L associated with a given normalized ENBW value is approximately given by:

$$L \approx \left[N(a_3 ENBW^3 + a_2 ENBW^2 + a_1 ENBW + a_0) \right] \quad (7)$$

where $[\cdot]$ denotes the operator rounding the argument to the nearest integer, while $a_3 = -1.46$, $a_2 = 2.16$, $a_1 = -0.22$ and $a_0 = -0.0007$. Further simulation results (not reported for the sake of brevity) show that if N exceeds about 120, the frequency responses as well as the ENBW values of the maximally-flat LPDs may sometimes differ enormously from those shown in Fig 1(b). A deeper analysis revealed that this is indirectly due to the fast growth of the coefficient values returned by (4), which may be affected by large numerical errors.

III. LPD Performance Comparison

In this Section, the performances of the windowing-based LPDs (obtained with the Hann window) and the maximally-flat LPDs are compared with one another for common values of $ENBW$ and impulse response length N. The parameters considered for performance comparison are:

- the *passband edge* defined as the frequency at which the LPD magnitude response reaches its peak before decreasing towards 0;
- the *passband RMS magnitude response errors* relative to the peak value of the magnitude response of the ideal LPD with the same ENBW.

It is worth emphasizing that *passband edge* as defined above is quite different from the classic -3dB bandwidth of typical filters. However, in Authors' opinion, the proposed bandwidth definition makes more sense in the case of LPDs, since it identifies clearly and unambiguously the frequency beyond which the FIR LPD frequency response deviates significantly (and definitively) from the ideal one.

Fig. 2(a)-(b) shows the magnitude responses of some windowing-based LPDs obtained with the Hann window and the corresponding maximally-flat LPDs, respectively, for $N = 100$ and for various normalized ENBW values. For the sake of comparison, the magnitude responses of two well-known full-band differentiators, namely the classic non-causal Euler finite difference with impulse response $h(n) = \frac{1}{2}[\delta(n+1) - \delta(n-1)]$ ($\delta(n)$ being the unit pulse) and the 5-point finite difference differentiator based on parabolic interpolation with impulse response $h(n) = \frac{1}{10}[2\delta(n+2) + \delta(n+1) - \delta(n-1) - 2\delta(n-2)]$, are plotted by using dashed and dash-dotted lines, respectively [17]. Observe that the frequency response of these full-band differentiators deviate considerably from the ideal one at frequencies not close to 0. Therefore, both the families of FIR LPDs considered exhibit a much better behavior than the full-band standard differentiators. At a glance, the magnitude responses of the maximally-flat LPDs are quite smoother than those of the windowing-based LPDs. Indeed, the former ones exhibit a broader transition band. This result suggests that, even if the output noise power is the same in both cases, the magnitude errors of maximally-flat LPDs at the passband edge are quite larger. This conclusion is confirmed by the results shown in Fig. 3(a)-(b), which depicts, on a logarithmic scale, the magnitude errors (relative to the peak value of the magnitude response of the ideal LPD with the same ENBW) of the same LPDs analyzed in Fig. 2(a)-(b). In both cases, the passband and stopband magnitude errors tend to decrease as the ENBW grows. However, while in the case of windowing-based LPDs the magnitude errors outside the transition bands exhibit ripples of comparable amplitude, the magnitude errors

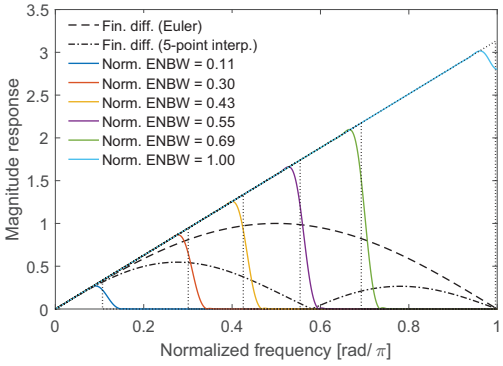

(a)

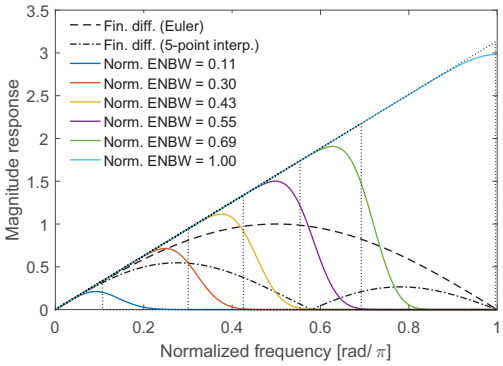

(b)

Fig. 2. Magnitude responses of some windowing-based LPDs obtained with the Hann window (a) and the maximally-flat LPDs (b) for $N = 100$ and for various normalized ENBW values. The dashed and dash-dotted lines refer to the classic Euler differentiator and the 5-point differentiator based on parabolic interpolation [17].

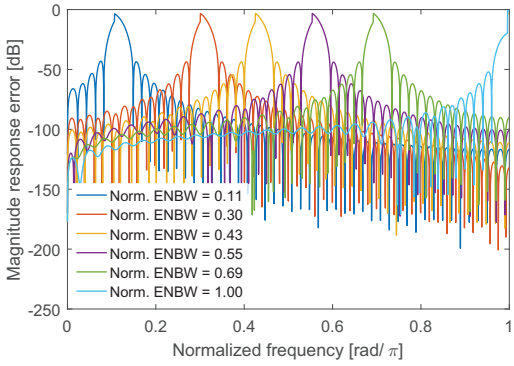

(a)

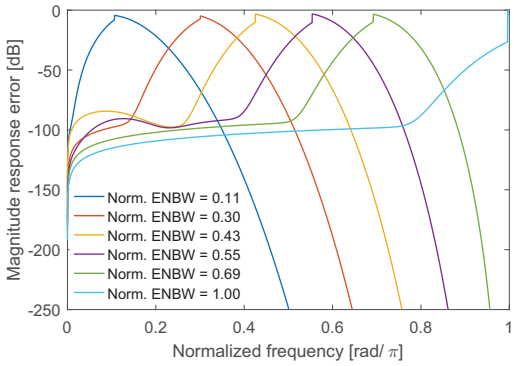

(b)

Fig. 3. Magnitude response errors (relative to the peak value of the magnitude response of an ideal LPD with respect to the ENBW) of some windowing-based LPDs obtained with the Hann window (a) and the maximally-flat LPDs (b) for $N = 100$ and for various normalized ENBW values.

of maximally-flat LPDs are much smaller in the stopband than in the passband, where, nonetheless, the flat behavior is clearly visible. Unfortunately, the corresponding transition bandwidth and the magnitude errors therein are much larger than those of windowing-based LPDs. Fig. 4(a)-(b) shows the relative offsets of the passband edge with respect to the ENBW for the windowing-based LPDs and the maximally-flat LPD, namely the difference between the passband edge of either filter (as defined at the beginning of this Section) and the corresponding ENBW, divided by the ENBW itself. Different curves refer to impulse responses of length $N = 40, 60, 80, 100$. In all cases, the passband edges are smaller than the filter ENBW by a few percent, as expected. Such relative offsets tend to decrease slightly as N grows and they are more severe (up to twice larger) in the case of maximally-flat LPDs especially for low ENBW values. On the contrary, as ENBW grows, the relative passband edge offsets decrease. The ratio between each pair of curves, for the same value of N, is roughly 2. This result confirms that the maximally-flat LPDs are less selective in frequency than those designed using the windowing method.

Fig. 5(a)-(b) reports the RMS magnitude response errors within the passband (relative to the peak magnitude of an ideal LPD) of the windowing-based LPDs and the maximally-flat LPDs for given values of normalized ENBW and impulse response length. Observe that, despite their maximally-flat behavior and lower sensitivity to the filter order, the passband RMS magnitude errors of the maximally-flat LPDs are always about 15-20 dB greater than those of the windowing-based LPDs.

IV. A Case Study: Power Systems Frequency Estimation

In this Section, the behavior of windowing-based and maximally-flat LPDs is analyzed and compared in a practical application scenario, i.e., voltage frequency estimation in AC power systems. This measurement problem can be addressed through a variety of techniques ranging from basic zero-crossing detection to advanced signal processing algorithms either in time or in the frequency domain [18]. Moreover, the need to monitor the power system frequency in real-time (especially over short time intervals) requires the use of the so-called Phasor Measurement Units (PMUs) [19]. In this respect, the most classic and simplest technique to determine the system frequency from synchrophasor data relies on the computation of the time derivative (normalized by 2π) of the unwrapped phase angles of the estimated voltage synchrophasor. This estimation approach (which is also described in Annex D of the IEC/IEEE Standard 60255:2018 [20]) suggests the adoption of a narrowband LPD rather than a traditional full-band differentiator to reduce the effect of disturbances affecting

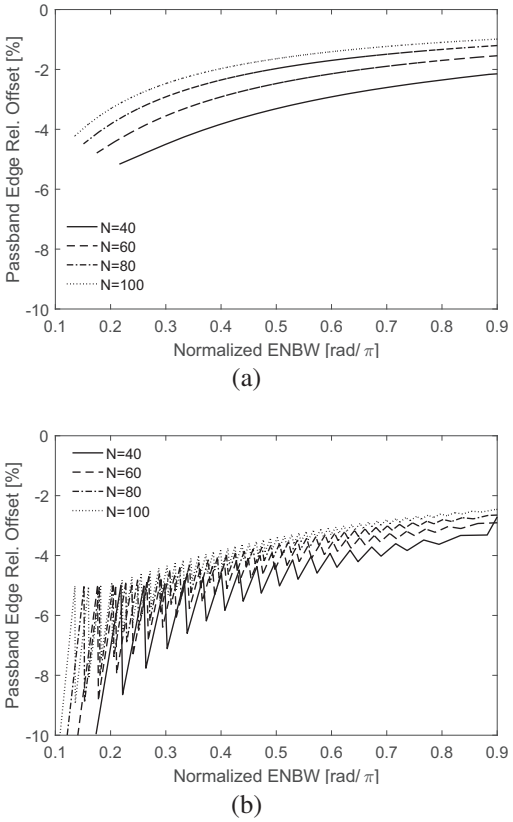

Fig. 4. Relative offset of the passband edge of the windowing-based LPDs obtained with the Hann window (a) and the maximally-flat LPD (b) with respect to the ENBW for impulse responses of length $N = 40, 60, 80, 100$.

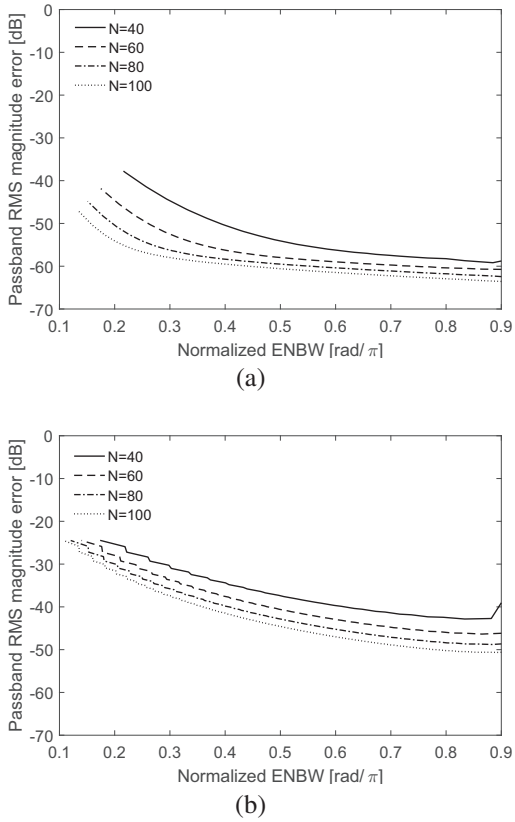

Fig. 5. RMS errors of the LPD magnitude response within the passband with respect to the peak magnitude of an ideal LPD with the same ENBW. In (a) and (b) the results of the windowing-based LPDs obtained with the Hann window and those related to the maximally-flat LPDs are plotted as a function of the normalized ENBW for impulse responses of length $N = 40, 60, 80, 100$.

power system waveforms [6]. To ensure a fair performance comparison, realistic conditions are simulated by estimating the synchrophasor phase angles with the down-conversion and filtering algorithm described in Annex D of the IEC/IEEE Standard 60255:2018 applied to a simulated 50-Hz voltage waveform (with a nominal amplitude of 1 p.u.) sampled at 6.4 kHz. Moreover, a special *Class M* equiripple low-pass FIR filter is used to minimize the impact of disturbances in worst-case conditions, as explained in [21]. The input simulated AC voltage is affected by:

- a static frequency offset of the waveform fundamental chosen at random in the range ± 5 Hz;
- 50 harmonics of amplitude up to 10% of the fundamental tone;
- a single 10% inter-harmonic interferer at 75 Hz;
- amplitude and phase modulation oscillations caused by sinusoidal components at 5 Hz with amplitude equal to 10% of the fundamental and 0.1 rad, respectively;
- wideband noise with Signal-to-Noise Ratio of 60 dB.

Most of the values listed above refer to the worst-case conditions reported in [20] for *Class M* PMU characterization, but in this example they are considered together. Fig. 6 shows the frequency estimation errors over half a second obtained by using (from top to bottom) the classic Euler finite difference, the 5-point finite difference differentiator based on parabolic interpolation, the windowing-based LPD and the maximally-flat LPD with $N = 110$ and normalized ENBW equal to 0.067, which is achieved for $L = 0$ (Indeed, for greater values of N, the coefficients returned by (4) tend to become numerically unstable as explained at the end of Section II-C). At a glance, both LPDs reduce the output power of disturbances by more than one order of magnitude as compared with the Euler differentiator and by a factor 4 with respect to the 5-point differentiator. Note also that the difference in the results returned by the two LPDs is minor in the case study considered. The approximately equal residual frequency error oscillations visible in both graphs are indeed due to the disturbances whose spectral content lies within the passband of both filters.

V. Conclusions

This paper reports a in-depth performance comparison of two families of FIR Low-pass Frequency Differentiators (LPDs), i.e. those designed by using the classic windowing method and those exhibiting a maximally-flat frequency response around DC obtained with recursive closed-form expressions. The purpose of this kind of digital filters is to estimate the derivative of input signals with a prevailing low-frequency spectral content with no phase distortion and without fur-

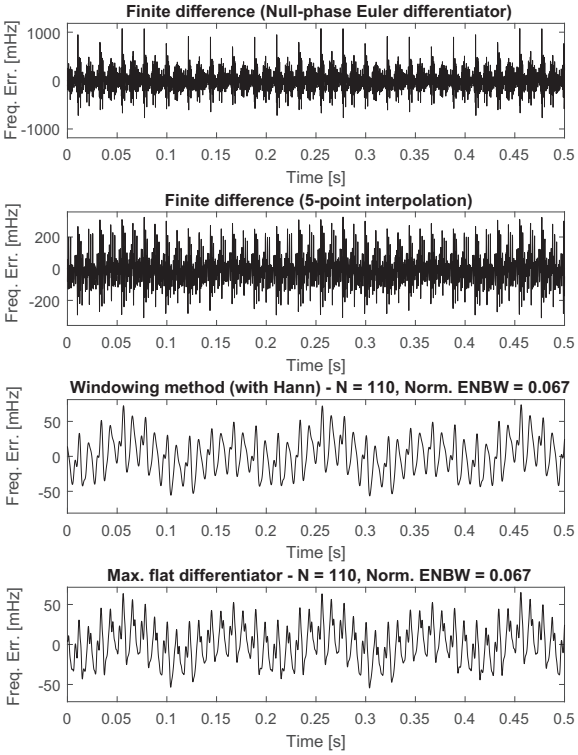

Fig. 6. Frequency estimation errors of a simulated noisy AC voltage waveform. The waveform frequency is estimated as the time derivative of the unwrapped synchrophasor phase angles estimated by a PMU, as explained in [21]. From top to bottom, the frequency error patterns refer to: the classic Euler finite difference, the 5-point differentiator based on parabolic interpolation, a windowing-based LPD and the maximally-flat LPD with the same length $N = 110$ and normalized ENBW equal to 0.067.

ther cascaded low-pass filters that introduce additional delays and processing burden. The maximally-flat LPDs are natively conceived to achieve very accurate derivatives around DC ensuring negligible magnitude response errors in the stopband. However, they exhibit a much broader transition band than the windowing-based LPDs as well as globally worse RMS and maximum magnitude errors within the passband. Moreover, the order of maximally-flat LPDs cannot be increased arbitrarily since the computation of the filter coefficients becomes numerically unstable as soon as the impulse response length exceeds about 120. However, it is possible that better performances can be obtained if design techniques based on numerical optimization are used. Finally, it is worth emphasizing that the criterion adopted for comparison and based on ENBW definition can be applied to other categories of LPDs, as well.

REFERENCES

[1] H. Fujioka, "Characterizing approximated differentiators in digital control," in *2010 11th International Conference on Control Automation Robotics Vision*, Singapore, Dec. 2010, pp. 923–926.

[2] C. Nayak, S. K. Saha, R. Kar, and D. Mandal, "An efficient and robust digital fractional order differentiator based ECG pre-processor design for QRS detection," *IEEE Trans. on Biomedical Circuits and Systems*, vol. 13, no. 4, pp. 682–696, Aug. 2019.

[3] Y. W. Nijim, S. D. Stearns, and W. B. Mikhael, "Lossless compression of seismic signals using differentiation," *IEEE Trans. on Geoscience and Remote Sensing*, vol. 34, no. 1, pp. 52–56, Jan. 1996.

[4] M. A. P. a. J. Platas-Garza and J. A. de la O Serna, "Dynamic phasor and frequency estimates through maximally flat differentiators," *IEEE Trans. on Instrumentation and Measurement*, vol. 59, no. 7, pp. 1803–1811, Jul. 2010.

[5] F. Messina, L. R. Vega, P. Marchi, and C. G. Galarza, "Optimal differentiator filter banks for PMUs and their feasibility limits," *IEEE Trans. on Instrumentation and Measurement*, vol. 66, no. 11, pp. 2948–2956, Nov. 2017.

[6] M. Rossi, "Reference system for the identification and acquisition of power system frequency transients," in *2019 IEEE 10th International Workshop on Applied Measurements for Power Systems (AMPS)*, Aachen, Germany, Sep. 2019, pp. 1–6.

[7] B. Kumar and S. C. Dutta Roy, "Design of digital differentiators for low frequencies," *Proceedings of the IEEE*, vol. 76, no. 3, pp. 287–289, Mar. 1988.

[8] M. Al-Alaoui, "Novel digital integrator and differentiator," *Electronics Letters*, vol. 29, pp. 376–378(2), Feb. 1993.

[9] H. L. Kennedy, "Improved IIR low-pass smoothers and differentiators with tunable delay," in *2015 International Conference on Digital Image Computing: Techniques and Applications (DICTA)*, Adelaide, Australia, Nov. 2015, pp. 1–7.

[10] M. A. Al-Alaoui, "Linear phase low-pass IIR digital differentiators," *IEEE Trans. on Signal Processing*, vol. 55, no. 2, pp. 697–706, Feb. 2007.

[11] O. Vainio, R. Lehto, and T. Saramaki, "Fractional-order FIR differentiators with optimum noise attenuation," in *Proc. IEEE Instrumentation Measurement Technology Conference*, Warsaw, Poland, May 2007, pp. 1–4.

[12] J. A. la O Serna and M. A. Platas-Garza, "Maximally flat differentiators through wls taylor decomposition," *Digital Signal Processing*, vol. 21, no. 2, pp. 183 – 194, 2011.

[13] I. W. Selesnick, "Maximally flat low-pass digital differentiator," *IEEE Trans. on Circuits and Systems II: Analog and Digital Signal Processing*, vol. 49, no. 3, pp. 219–223, Mar. 2002.

[14] D. Belega, D. Petri, and D. Dallet, "Frequency estimation of a sinusoidal signal via a three-point interpolated dft method with high image component interference rejection capability," *Digital Signal Processing*, vol. 24, no. 1, pp. 162 – 169, 2014.

[15] D. Belega and D. Petri, "Frequency estimation by two- or three-point interpolated fourier algorithms based on cosine windows," *Signal Processing*, vol. 117, pp. 115 – 125, 2015.

[16] Soo-Chang Pei and Peng-Hua Wang, "Closed-form design of maximally flat fir hilbert transformers, differentiators, and fractional delayers by power series expansion," *IEEE Trans. on Circuits and Systems I: Fundamental Theory and Applications*, vol. 48, no. 4, pp. 389–398, Apr. 2001.

[17] F. Scheid, *Numerical Analysis*. McGraw-Hill Education - Shaum's series, 2nd edition, 1989.

[18] P. M. Ramos and A. C. Serra, "Comparison of frequency estimation algorithms for power quality assessment," *Measurement*, vol. 42, no. 9, pp. 1312 – 1317, 2009.

[19] A. G. Phadke and T. Bi, "Phasor measurement units, wams, and their applications in protection and control of power systems," *Journal of Modern Power Systems and Clean Energy*, vol. 6, no. 4, pp. 619–629, Jul. 2018.

[20] "IEEE/IEC International Standard - Measuring relays and protection equipment - Part 118-1: Synchrophasor for power systems - Measurements," *IEC/IEEE 60255-118-1:2018*, pp. 1–78, Dec. 2018.

[21] D. Macii and D. Petri, "Digital filters for phasor measurement units: Design criteria, advantages and limitations," in *Proc. IEEE International Workshop on Applied Measurements for Power Systems (AMPS)*, Aachen, Germany, Sep. 2019, pp. 1–6.